Physica Medica (2012) **28**, 94–108

Available online at www.sciencedirect.com

SciVerse ScienceDirect

journal homepage: http://intl.elsevierhealth.com/journals/ejmp

REVIEW PAPER

Iterative reconstruction methods in X-ray CT

Marcel Beister, Daniel Kolditz, Willi A. Kalender*

Institute of Medical Physics (IMP), Unversity of Erlangen-Nürnberg, Henkestraße 91, 91052 Erlangen, Germany

Received 28 November 2011; received in revised form 12 January 2012; accepted 15 January 2012
Available online 10 February 2012

KEYWORDS
CT;
Image reconstruction;
Iterative reconstruction;
Statistical reconstruction;
Model-based reconstruction;
Dose;
Image quality

Abstract Iterative reconstruction (IR) methods have recently re-emerged in transmission x-ray computed tomography (CT). They were successfully used in the early years of CT, but given up when the amount of measured data increased because of the higher computational demands of IR compared to analytical methods. The availability of large computational capacities in normal workstations and the ongoing efforts towards lower doses in CT have changed the situation; IR has become a hot topic for all major vendors of clinical CT systems in the past 5 years.

This review strives to provide information on IR methods and aims at interested physicists and physicians already active in the field of CT. We give an overview on the terminology used and an introduction to the most important algorithmic concepts including references for further reading. As a practical example, details on a model-based iterative reconstruction algorithm implemented on a modern graphics adapter (GPU) are presented, followed by application examples for several dedicated CT scanners in order to demonstrate the performance and potential of iterative reconstruction methods. Finally, some general thoughts regarding the advantages and disadvantages of IR methods as well as open points for research in this field are discussed.

Introduction

Iterative reconstruction (IR) methods have re-emerged in transmission x-ray computed tomography (CT). This initial statement reflects the fact that the concept of iterative reconstruction, which was already established in single-photon emission CT in the 1960s [1], was also used in the first transmission CT efforts in the early 1970s [2]. They were successfully used in the first clinical CT products when relatively small amounts of measured data were generated per scan and reconstructed into crude 128 × 128 image matrices. They were not practical for fast high-resolution CT with 512 × 512 or finer image matrices and were only used in special research efforts, e.g. for investigating their potential in metal artifact reduction [3], noise reduction, uncommon trajectories or incomplete data, when long reconstruction times were not a limiting factor.

The availability of large computational capacities in normal workstations and the ongoing efforts towards lower doses in CT have changed the situation; IR has become a hot

* Corresponding author. Tel.: +49 9131 85 22310; fax: +49 9131 85 22824.
E-mail address: willi.kalender@imp.uni-erlangen.de (W.A. Kalender).

1120-1797/$ - see front matter
doi:10.1016/j.ejmp.2012.01.003

topic for all major vendors of clinical CT systems in the past years. First products with regulatory approvals in Europe and the USA are already available and will be addressed in Section: "Application examples". While analytical algorithms such as the commonly used filtered back projection (FBP) are based on only a single reconstruction, iterative algorithms use multiple repetitions in which the current solution converges towards a better solution. As a consequence, the computational demands are much higher. Due to the exponential growth of computer technology proposed by Moore's law, which is holding since the 1970s, and the computational capacities available in a modern processor (central processing unit, CPU) or graphics adapter (graphics processing unit, GPU) the usage of IR methods has become a realistic option with reconstruction times acceptable for clinical workflow. Nevertheless, new algorithmic innovations are needed because computational demands have increased due to the fact that image resolution was improved, acquisition times were greatly reduced, dual-source scans became part of the clinical routine and modern IR algorithms gained additional complexity. Iterative reconstruction algorithms may allow a notable dose reduction due to a more precise modeling of the acquisition process. This is expected to support the trend towards continued dose reduction, which is considered a necessity in view of the increasing number of CT examinations in clinical routine [4,5]. In addition, iterative methods with the ability to include various physical models represent a more intuitive and natural way of image reconstruction. Statistical reconstruction methods, for example, model the counting statistics of detected photons by respective weighting of the measured rays. Other implementations include the modeling of the acquisition geometry or incorporate further information on the x-ray spectra used for improving the simulation of the acquisition process.

So far, the renaissance of IR methods has led to vendor-specific solutions only provided as "black boxes" with very little information on algorithmic principles and details. This may partly be due to the increased complexity of the algorithms, the time-consuming parameterization of the internal model and the fact that a noteworthy dose reduction is a proprietary and valuable competitive sales argument.

This work strives to provide more detailed information on IR methods and aims at physicists and physicians already active in the field of CT who want to know more about the basic principles behind IR methods. We intend to give an overview on the terminology used and introduce the most important algorithmic concepts including references for further reading in Section: "Overview of algorithmic concepts". As a practical example we present details on a model-based iterative reconstruction algorithm in Section: "Implementation of a model-based iterative reconstruction" for the interested reader. Application examples are given in Section: "Application examples" to demonstrate the performance and potential of model-based iterative reconstruction methods both for clinical CT and for CT in general using examples of several dedicated CT scanners. We conclude with some general thoughts regarding the pros and cons of iterative reconstruction methods in Section: "Discussion".

Overview of algorithmic concepts

This section will give an overview of available iterative reconstruction methods and the range of physical models which can be applied in these algorithms. In the literature a large number of acronyms can be found; some important abbreviations for algorithms and terms used in this field are shown in Table 1. Unfortunately these abbreviations are not always used consistently in the literature and a number of variations and combinations of different concepts exist. We distinguish between pure iterative methods without any modeling, statistical methods with modeling of the photon counting statistics, and model-based methods which go beyond statistical modeling.

Iterative methods

All iterative reconstruction methods consist of three major steps which are repeated iteratively as visualized in Fig. 1. First, a forward projection of the volumetric object estimate creates artificial raw data which, in a second step, are compared to the real measured raw data in order to compute a correction term. In the last step the correction term is back projected onto the volumetric object estimate. The iteration process can be initiated with an empty image estimate or using prior information, for example, a standard FBP reconstruction or a volume of a similar object. In general, the better the prior images match the final images, the faster the process converges towards a stable solution. The iterative process is finished when either a fixed number of iterations is reached, or the update for the current image estimate is considered small enough or when a predefined quality criterion in the image estimate is fulfilled. Unfortunately, a general rule of thumb for a termination criterion which exits early enough to avoid unnecessary computations and still guarantees

Table 1 Selection of the most prominent iterative reconstruction algorithms and references to initial or important publications.

Abbreviation	Meaning	Reference
ART	Algebraic reconstruction technique	[6]
SART	Simultaneous ART	[8]
SIRT	Simultaneous iterative reconstruction technique	[12]
OS-SIRT	Ordered subset SIRT	[12,13]
MART	Multiplicative algebraic reconstruction technique	[6,14,15]
ML-EM	Maximum likelihood expectation-maximization	[9]
OS-EM	Ordered subset expectation-maximization	[11]
OSC	Ordered subset convex algorithm	[27–29]
ICD	Iterative coordinate descent	[30–32]
OS-ICD	Ordered subset ICD	[34,35]
MBIR	Model-based iterative reconstruction	[32,36]

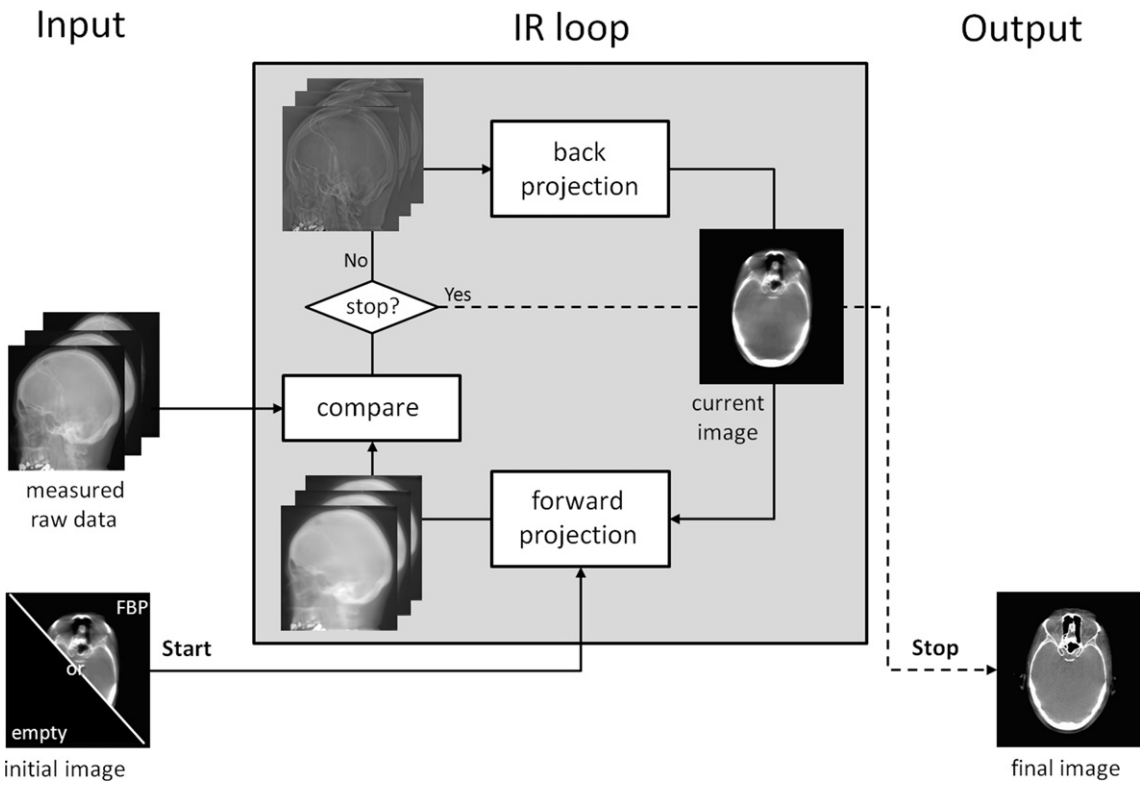

Figure 1 Schematic view of the iterative reconstruction process. The volume estimate is initiated either with an empty image or, if available, with a prior volume from e.g. an FBP reconstruction. First, a forward projection of the current volumetric image is necessary to create artificial raw data. Then artificial and measured raw data are compared and an updated image is computed which subsequently is backprojected to the current volumetric image. These three steps form the IR loop. If a stop criterion is matched, the loop is terminated and the current volumetric image becomes the final volumetric image.

a satisfactory image quality is hard to give and often depends on the properties of the reconstructed dataset.

The simplest form of iterative reconstruction is the algebraic reconstruction technique (ART) [6], which was already used for the reconstruction of images in the first CT systems [2]. ART is based on Kaczmarz' method [7] for solving linear systems of equations $Ax = b$, where in terms of image reconstruction x are the voxels of the volume to be reconstructed, A is the system matrix used for producing the raw data and b are the pixels of the measured raw data. The entries of the matrix A correspond to rays from the x-ray source through the volume to the detector pixels, i.e. the line integral of the linear attenuation coefficient. Often a positivity constraint is applied to the voxels based on the assumption that negative attenuation values are not possible. While the original ART algorithm works on single rays and thus single pixels, the simultaneous algebraic reconstruction technique (SART) [8] performs updates for complete raw data projections. This leads to a much faster convergence of volumetric images towards a stable solution, but a relaxation factor becomes necessary to keep the noise low and to reduce problems with streak artifacts.

The idea of using ordered subsets (OS) to reduce the reconstruction times further was originally proposed for emission tomography [9,10] and was transferred to transmission methods some years later [11]. In OS-based methods, the projection data is divided into groups called subsets and the update is performed for each group instead for the complete set of available projections. The convergence speed increases with number of subsets, i.e. for smaller numbers of projections per subset. But the potential for overcorrection is increasing, leading to higher noise or possibly artifacts. The idea of OS was applied to SIRT (simultaneous iterative reconstruction technique) [12,13] leading to the OS-SIRT method, with SART being one extreme with only one projection per subset and SIRT being the other extreme with only one subset containing all the projections. MART methods (multiplicative algebraic reconstruction technique) [6,14,15] are multiplying the update term onto the current solution in contrast to all previously mentioned methods which are adding (or subtracting) the update term. In general all ART-based methods are non-statistical and model the geometry of the acquisition process better than common analytical methods based on FBP, which assume a continuum of acquisition positions. Therefore ART-based methods can better deal with sparse data and an irregular sampling of acquisition positions.

Statistical methods

The key idea of statistical methods is to incorporate counting statistics of the detected photons into the reconstruction process. In transmission CT the number of photons leaving the x-ray tube as well as the measured

photons at the detector, which passed through the patient or object, are assumed to be Poisson distributed. While this assumption seems to be valid in most cases, the situation for acquisitions with very low dose is not clear because effects in the detector such as electronic noise are gaining importance compared to the distribution of the photons arriving at the detector [16]. Statistical reconstruction methods can work in three different domains: in the domain of the raw data projections (sinogram domain), in the domain of the volumetric images (image domain) or during the iterative reconstruction process. The main advantage of methods working in either the raw data or the image domain is that they are independent of the reconstruction algorithm; therefore they are often considered pre- and post-processing methods which use information based on a physical model. This has advantages in terms of computational speed, but of course there are also limitations to the physical model (compare Section: "Physical modeling").

Methods in the raw data domain

The methods working in the raw data domain apply an adaptive or iterative 2D edge-preserving denoising algorithm directly on the projection raw data [17,18,19,20,21]. Most algorithms are assuming a Poisson distribution of the detected photons and adaptively filter regions with higher attenuation more strongly due to the larger uncertainties compared to regions with lower attenuation; this is based on physics considerations. The subsequent reconstruction using the noise-reduced data can be done with either a common FBP reconstruction or an iterative method, which leads to a noise reduction in the volumetric images. Since raw data projections are directly altered, this always involves the risk of losing structures or spatial resolution depending on the filtration method and strength.

Methods in the image domain

Algorithms in the volumetric image domain are denoising the volume after the reconstruction and, again, they are aiming for noise reduction while preserving spatial resolution. Additional information, such as photon statistics derived from raw data projections, may be used for selective smoothing in the image data [22,23]. All filters which are applied on the reconstructed volumetric data without using any information on the acquisition process (compare Section: "Prior object information modeling") are not considered statistical reconstruction methods, but post-processing filters.

Full statistical methods

Full statistical methods as part of the reconstruction process have their roots in the reconstruction algorithms for emission tomography, specifically for positron emission tomography (PET) and single-photon emission computed tomography (SPECT). Full statistical reconstruction algorithms can be roughly divided into two groups: Methods based on or correlated to the maximum likelihood (ML) principle and those based on or correlated to the least squares (LS) principle. They all somehow model the statistics of photons during acquisition and can thus provide reduced noise in the volumetric images compared to non-statistical methods. The likelihood is the hypothetical probability that an event which has already occurred would yield a specific outcome. By maximizing the likelihood, the reconstruction algorithm tries to find the set of parameters that makes the measurements the most probable. In maximization methods the natural logarithm of the likelihood (log-likelihood) is often more convenient, which fortunately has its maximum values at the same points as the function itself.

The maximum likelihood expectation-maximization (ML-EM) algorithm [24] for emission tomography was adapted to transmission tomography in 1984 [9] and consists of two alternating steps: An E-step, which computes the expectation of the log-likelihood, and an M-step, which finds the next estimate through maximizing the expected log-likelihood. The ordered subset principle was ported to ML-EM transmission tomography forming the OS-EM-based algorithms [11] which allows a significantly faster convergence. The convex algorithm introduced in 1990 [25] is closely related to ML-EM and thus also based on the maximum likelihood principle, but converges much faster than classical ML-EM for transmission tomography without ordered subsets [26]. Again the ordered subset principle was applied to this algorithm [27,28,29], leading to the ordered subset convex algorithm (OSC), which has significantly faster convergence compared to the original convex algorithm and allows for easy parallelization.

The least squares principle represents a second and alternative approach to statistical reconstruction and methods based on iterative coordinate descent (ICD) [30,31,32,33] were proposed and successfully implemented for transmission tomography. They are hard to parallelize for multiple CPU or GPU threads since single pixels or coordinates are iteratively updated to minimize a cost function, but show a very rapid convergence when, for example, initialized with a volume from an FBP reconstruction [31]. Implementations based on ordered subsets with faster convergence (OS-ICD) were also published [34,35].

Model-based methods

Here the term "model-based" classifies all methods which go beyond modeling statistics of the detected photons as Poisson distributed; of course, statistical methods can alternatively also be classified as a subset of model-based methods. This separation was chosen due to the term "statistical reconstruction" being very common in the literature. The abbreviation MBIR (model-based iterative reconstruction) is a general designation for all model-based methods since it neither defines the aspects of the modeling nor their implementation [36]. In general, model-based methods try to model the acquisition process as accurately as possible. The acquisition is a physical process in which photons with a spectrum of energies are emitted by the focus area on the anode of an x-ray tube. Subsequently they travel through the object and are either registered within the area of a detector pixel, scattered outside of the detector or are absorbed by the object. The better a forward projection is able to model this process, the better the artificial image can be matched to the acquired raw data. Better matching artificial raw data lead

to better correction terms for the next update step and, in consequence, to an improved image quality in the reconstructed data. While in theory many physical effects can be modeled up to a certain degree, a fair balance between algorithmic and computational complexity and improvements in image quality is always required. Otherwise computational demands may rise to unacceptable levels. This should be kept in mind and this is also the reason why many effects are currently not modeled in available model-based implementations.

Geometric modeling

In geometric modeling, the acquisition system and the volumetric images are modeled as three dimensional objects. In most reconstruction methods both the focal spot of the x-ray tube as well as each pixel of a detector are assumed to be infinitely small points instead of areas with a defined extent. Also, each voxel is considered as an infinitely small point which, of course, does not reflect reality well. The error introduced for not modeling a voxel with three dimensional (3D) extents strongly depends on the resolution of the reconstructed volumetric images compared to the maximum possible resolution of the acquisition system. If the size of voxels is too large and the sampling thereby too coarse for the scan geometry, noise can increase with a destination-driven (voxel-driven) backprojection when information of some pixels is either completely omitted during backprojection or only information of a single pixel is used although multiple pixels should contribute to the back projected voxel. A source-driven (ray-driven) backprojection does not suffer from this effect, but is also computationally more expensive. In FBP-based methods a row-wise convolution with a selectable kernel is applied to the raw data. Thus, a kernel can also incorporate a spatial frequency emphasis for high or low frequencies and allows to trade noise for resolution, which can compensate for some of the described effects [5]. In addition a column-wise smoothing can be applied to improve the data usage within the reconstruction, which leads to reduced image noise while at the same time degrading spatial resolution. This is essentially image-based smoothing without using a physical model (compare Section: "Methods in the raw data domain"). Iterative reconstruction methods are all based on sequential forward and back projections which form the surrogate acquisition and the update component (see Fig. 1). If both steps are not matching very closely, the iterative reconstruction will continuously try to correct for inconsistencies and thereby cause even more inconsistencies. Modeling the focal spot size of the x-ray tube and the extents of the detector pixels allows the reconstruction to avoid having inconsistencies between surrogate and measured data which otherwise cannot be corrected for. Including geometric extent in the computation of artificial projection data requires improvement of the forward projection. All methods can be separated into two groups: source-driven methods, which essentially project each voxel as either a 3D box or a blob (often a sphere) onto the detector image [32,37,38,39] and destination-driven methods, which cast one or multiple rays from the detector pixel position to the x-ray source and sum up values of the intersected voxels [40,41,42,43]. Destination-driven multi-ray methods have already been used for emission tomography image reconstruction for example in SPECT [44] and PET [45]. They cast multiple rays and average their results to approximate the geometric extents of source and destination.

Physical modeling

In physical modeling the interactions of photons in the measured object are addressed. Most reconstruction methods model the acquisition only as a linear process in which all photons have the same energy and are either attenuated or survive by a certain percentage. In reality the energy spectrum of x-ray tubes is always polychromatic and non-linear effects such as scatter or beam hardening also have a significant impact on the measured intensities, which results in cupping artifacts and dark areas surrounding objects of dense or high-Z materials. If such effects are modeled in the reconstruction process, these artifacts can be reduced to a large degree without any heuristic correction methods. Methods can either use normal or logarithmic intensities. While the former are more complicated due to the nonlinearity introduced by the physical processes, the latter are only approximations and ignore beam hardening effects. The major problem with physical modeling is that knowledge on the material composition of each voxel is required and that this information cannot be provided by a standard CT reconstruction. There are essentially two ways of dealing with this problem: If there is prior knowledge on the materials in the scanned object, segmentation based on a common FBP reconstruction can be done either using thresholds or using information from dual energy CT. Spectral information on the photons emitted by the x-ray tube is a further required component for physical modeling. This can either be measured directly at the modality or approximated using information on tube voltage and pre-filtration [46].

If a shaped filter is used or if the anode heel effect is modeled, the spectra become dependent on the angular position in relation to the central ray, which, of course, needs to be included in the model. The third component which influences the detected photons is the detector itself. To include this into the physical model, information on the absorber material is required as a minimum. The interactions of photons in the measured object are dominated by three different physical effects: photo electric effect, Compton scattering and Rayleigh scattering. Various approaches have been presented in order to approximate the energy-dependent attenuation and the problem of insufficient information on the material compositions [47,48,49]. X-ray beams can be modeled polychromatic by dividing the spectrum into a number of energy bins and computing each interaction within a voxel for each bin. But the computational expense would be very high and the success, of course, depends on the validity and accuracy of spectral modeling. Scattering is a process where photons are leaving their original straight trajectory and might interact multiple times within the measured object; tracing single rays through the object is not sufficient when scatter is to be taken into account. Such computationally complex problems are usually modeled by using Monte Carlo methods which approximate the overall result by simulating a large amount of photons and choosing interactions based on probabilities. Although these methods have been

implemented on modern GPUs, clusters and computation clouds, the computation times are still very high compared to the desired reconstruction times and are not yet considered a realistic option as a source of information during iterative reconstruction.

Prior object information modeling

Prior object information can be used to correct for unrealistic situations in the estimated volumetric image during the iterative reconstruction process, which is often referred to as regularization. This includes, for example, a positivity constraint on the reconstructed attenuation values or smoothing out differences between neighboring voxels which, based on the prior model information, are considered unrealistic. Regularization based on prior information between iterations can lead to faster converging towards a solution which better fits the measured objects material properties. The goal of all regularization algorithms is to reduce the noise while preserving the spatial resolution. There is a wide range of 3D noise-filter algorithms based on bilateral filters [50], non-local means [51], total variation minimization [52,53,54] or Markov random fields with quadratic and non-quadratic roughness penalty functions as well as convex and non-convex sparsity penalty functions [55]. The main problem of all regularization algorithms is the choice of parameters and their influence on both convergence and final volumetric image. All edge-detecting algorithms are non-linear processing methods which can introduce new artifacts if, for example, the algorithm detects and preserves an edge, although the "edge" was only caused by noise. In addition, if the filter was chosen too strong, edges might be removed or the resulting volumetric images can be perceived as unrealistic. Thus regularization is often skipped or reduced towards the end of the reconstruction process.

Implementation of a model-based iterative reconstruction

In this section, details on a generalized model-based iterative reconstruction algorithm which was implemented for modern GPUs are provided. Normal processors (CPUs) are optimized for computations in a serial fashion by using complex branch prediction strategies and by spending large amounts of transistors for caches to hide memory latencies. In contrast, GPUs are optimized for highly parallel computations as required in 3D computer graphics and hide memory latencies by having a work queue with many parallel tasks. Therefore, a GPU can spend much more transistors on arithmetic logic units which lead to a peak computational performance an order of magnitude higher compared to CPUs. GPU computing has gained great attention for scientific computations, for example in medical image processing and data reconstruction. Both forward and backprojection can be easily divided into many data parallel tasks, thus iterative reconstruction algorithms can profit greatly from the highly parallel architecture of GPUs. Our implementation uses the CUDA framework from NVIDIA (Compute Unified Device Architecture, NVIDIA Corporation, Santa Clara, USA); a vendor-independent framework for GPU computing called OpenCL is also available. The iterative reconstruction method was integrated into our existing hybrid GPU-CPU reconstruction framework. The proposed MBIR method models three different aspects: Detected photons are assumed to be Poisson distributed; the focal spot as well as detector pixels are modeled to have 2D extents; image voxels are modeled to have 3D extents; and regularization accounts for unrealistic variations between neighboring voxels due to prior object information. The proposed MBIR algorithm was applied to data sets of a C-arm-based flat-detector CT (FDCT), a simulation of a dedicated CT of the breast and a micro-CT system. Examples of the results are presented in Section: "CT in general" of this article.

Photon statistics modeling

In model-based algorithms photon statistics considerations are important aspects for possible dose reduction. Here we chose the proposed iterative method to be based on the ordered subset convex algorithm [29] (see Section: "Full statistical methods"). There are multiple reasons for this choice: The OSC algorithm shows a fast convergence towards a stable solution if the subset size is chosen reasonably, allows for a good parallelization, which is very important for an efficient implementation on a massively parallel GPU architecture and offers a high potential for dose reduction [56]. In OS algorithms only a subset of all projections is employed for updating the image estimate in multiple subsequent steps. After the estimate has been updated during a given step, a different subset is chosen and the updates are performed on the new volumetric image, resulting in multiple updates during a single iteration. The subsets were chosen such that the angles between the projections in a subset were equal. The order of the subsets was varied from iteration to iteration by choosing the first subset randomly. All subsequent subsets were chosen to close the largest gap and to maximize the angular distance to the previous chosen subset (compare [29,57]). The update process can be formulated as an equation: if K denotes the total number of iterations and k the current iteration number, then each iteration is divided into a number of subsets s_k such that each subset visits N_p/s_k projections, with N_p being the total number of projections. We define the total subset counter v that counts through all subsets of all iterations. In addition we define the subset Radon transform operator R_v that corresponds to the forward projection of subset v and R_v^T describes the back projection of subset v. R_v consists only of those lines of R that are contained in subset v. The attenuation values of the acquired raw data projections are denoted as p. The update from subset v to subset $v+1$of the image estimate f_v can be described as:

$$f_{v+1} = f_v + f_v \frac{R_v^T\left(e^{-R_v f_v} - e^{-p}\right)}{R_v^T\left(e^{-R_v f_v} \cdot R_v f_v\right)} \tag{1}$$

A closer look at the formula reveals that three instances of the volumetric image need to be present in parallel during operation. One instance is the current image estimate f_v used for creating surrogate raw data ($R_v f_v$) and for applying the update term in the fraction. In addition, two

instances for the numerator and denominator of the update term are necessary, since these are computed for all projections of the subset s_v before the fraction and the multiplication with the current estimate is computed. The OSC algorithm consists of four major steps: First, surrogate raw data is computed and converted from attenuation to intensity values ($e^{-R_v f_v}$). In a second step, the numerator is computed by backprojecting the difference of surrogate intensities and measured intensities e^{-p} and adding it to the numerator volume. In a similar third step the product of surrogate intensities and surrogate attenuation is back-projected and added to the denominator volume. In a final step the numerator volume is divided by the denominator volume, multiplied with the current estimate and added to the current estimate in order to form a new estimate for the next subset iteration.

Geometric modeling

Besides modeling photon statistics, our approach also models the most important geometrical parameters (see Section: "Geometric modeling") such as the volumetric extent of each image voxel, the area of the detector pixels as well as the area of the focal spot. For the modeling of both forward and back projection, a multi-sampling approach was chosen, which approximates the volumetric extent of the x-ray beam leaving the tube, going through the voxels and arriving at detector elements by sending multiple rays within the volumetric extent and averaging the resulting integrals. The principle of multi-sampling is shown in Fig. 2. This approach was chosen mainly due to computational performance reasons: A destination-driven forward projection allows good parallelization for a GPU by creating one thread per detector pixel. This leads to parallel read-only access on the volumetric image data and to single thread read-write access for the surrogate projection data. All source-driven approaches require parallel read-write access to the surrogate projection data, which makes methods for avoiding competitive race conditions mandatory and, in consequence, lead to a serious decrease in computational performance. Source-driven methods that perform a volumetric modeling are projecting a two-dimensional footprint of the voxel onto the raw data [32,37,38,39], which additionally increases the parallel write access penalty. Since no efficient GPU-based solution has been proposed up to date and the sampling approach allows a straightforward implementation with sufficient performance, the decision was made in favor of the latter. The situation for the back projection is quite similar to the image voxels being the destinations and the detector pixels the sources. Again a destination-driven approach allows good parallelization for a GPU by creating one thread per image voxel avoiding concurrent write access to voxels.

In the destination-driven forward projection used here, the physical size of the detector pixels is simulated by sending rays from multiple evenly distributed positions on the detector within a single detector element. The focus position is multi-sampled choosing multiple points on, for example a nominal rectangular area. For simplicity, all points here are assumed to be evenly distributed in a rectangular area, but different shapes of the focus area and sampling patterns representing the physical distribution of photons on the anode of the x-ray tube are also possible if respective information is available. The ray integrals are

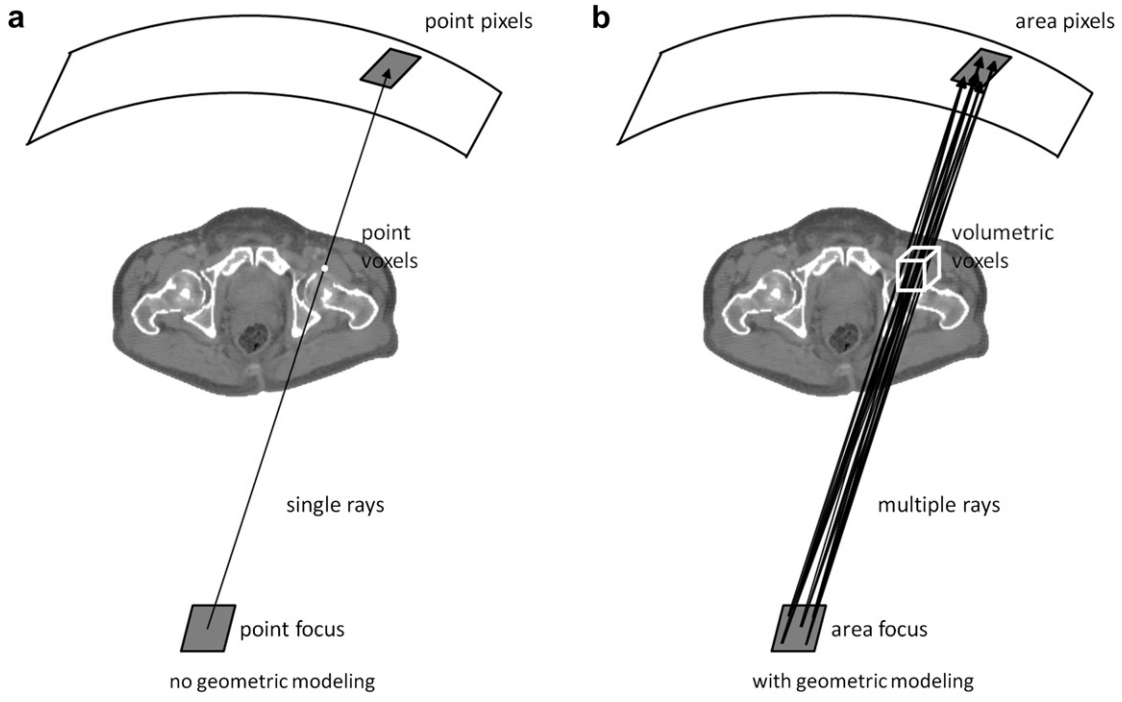

Figure 2 Example of standard FBP without geometric modeling (a) and MBIR algorithm with geometric modeling (b). In this example the volumetric extent is modeled using a multi-sampling approach in which rays from all sampling points on the focus are sent through the volume towards all sampling positions on the detector pixel area.

computed using the interpolation method of Siddon [42], which considers the extent of voxels by weighting the contribution of each voxel by the length of the ray through this voxel. Rays are sent from all sampling positions on the detector pixels through the voxels to all sampling positions on the focal spot. The mean value of all line integrals is stored as the surrogate pixel value. The back projection is implemented as a voxel-driven algorithm, which multi-samples the focus position by creating multiple coordinate transformation matrices for points on a rectangular area parallel to the detector orientation identical to the sampling used for the forward projection. While iterating through all voxels, the voxels' geometric volume is multi-sampled by performing the back projection on multiple positions within the physical three dimensional extent of the voxel. For all combinations of coordinate transformation matrices and voxel samples a value is read from the update projection data and the mean value is added to the voxel's current value.

Prior object information modeling

To account for unrealistic variations between neighboring voxels (see Section: "Prior object information modeling"), a regularization technique based on total variation (TV) minimization is applied during the iterative process. This principle was introduced for image processing purposes by Rudin, Osher and Fatemi (ROF) in 1992 [52]. TV minimization is a non-linear method which has the advantage of reducing noise while preserving sharp edges. By minimizing the derivative of the image data, the benefit of eliminating single peaks is higher compared to smoothing out borders of edges. The discrete TV semi-norm used for an image $u_{i,j}$ of size $m \times n$ is

$$\mathrm{TV}(u) = \sum_{\substack{1 \le i \le m \\ 1 \le j \le n}} \left\| (\nabla u)_{i,j} \right\|_2 \tag{2}$$

with

$$(\nabla u)^1_{i,j} = \begin{cases} u_{i+1,j} - u_{i,j}, & i < m \\ 0, & i = m \end{cases}$$

$$(\nabla u)^2_{i,j} = \begin{cases} u_{i,j+1} - u_{i,j}, & j < n \\ 0, & j = n \end{cases} \tag{3}$$

The denoising problem is often formulated as an unconstrained minimization problem which uses the TV term as a Tikhonov regularization (Ω denotes the image domain, usually a rectangle in $\mathbb{R}^2$ to model an image, f is the input image, $|\cdot|_2$ is the Euclidean norm on that domain and λ is a regularization parameter to control the strength of the regularization):

$$\mathrm{TV}_{min} = \min_u \left\{ \int_\Omega |\nabla u|_2 + \frac{\lambda}{2} \|u - f\|_2^2 \right\} \tag{4}$$

Due to the L^2 norm of the data fidelity term in Eq. (2), low-contrast regions will be removed, while strong contrast regions are kept. For data sets with low-contrast details it is useful to use a contrast invariance L^1 data fidelity term instead [58]. Duality-based methods which make use of the dual formulation of the ROF model have shown a greatly improved computational performance [53,59,60], thus our CUDA implementation of the TV minimization uses the duality-based algorithm described by Zhu et al. [53]. It consists of a dual step for the gradient ascent and a primal step for the gradient descent. Subsequently the duality gap is computed and the iteration is finished if the gap falls below the predefined threshold or the maximum number of iterations is reached. Due to GPU memory limitations, denoising is always performed subsequently on two-dimensional slices. From iteration to iteration the algorithm switches between lateral, coronal and sagittal slices to avoid favoring one dimension.

Application examples

Up to now the focus of IR developments and applications has been on modern clinical CT, i.e. on multi-slice spiral CT whole body applications, and they were driven almost exclusively by the major CT manufacturers. Impressive results are available for this sector and will be described in Section: "Clinical CT". However, iterative reconstruction algorithms can be applied universally to image reconstruction in all kinds of CT. In Section: "CT in general" we illustrate this by examples for three special CT scanners dedicated to interventional CT, breast CT and micro-CT.

Clinical CT

By the end of 2011, the four major CT vendors had all presented their IR products as summarized in Table 2. GE Healthcare started with ASIR (adaptive statistical iterative reconstruction) in 2008; it was followed by a more complex model-based iterative reconstruction method initially called MBIR and re-named to VEO when presented as a product. Siemens presented IRIS (image reconstruction in image space) in 2009 and currently promotes SAFIRE (sinogram affirmed iterative reconstruction), a reconstruction method which works in both raw data and image space. Philips introduced their iterative reconstruction iDose at RSNA 2009 which aims at producing a noise appearance with

Table 2 List of statistical reconstruction software products of major vendors of clinical CT systems and the year of introduction.

Acronym	Meaning	Vendor	Year
ASIR	Adaptive statistical iterative reconstruction	GE	2008
VEO (MBIR)	(Product name)	GE	2009
IRIS	Image reconstruction in image space	Siemens	2009
SAFIRE	Sinogram affirmed iterative reconstruction	Siemens	2010
iDose	(product name)	Philips	2009
AIDR	Adaptive iterative dose reduction	Toshiba	2010

respect to structure and spectrum similar to FBP results. Toshiba introduced their AIDR (adaptive iterative dose reduction) software in the USA in 2010.

Unfortunately the publications regarding these manufacturer solutions mostly relate to the comparison of a "black box" algorithm, the manufacturer's proprietary solution, to the standard analytical FBP approach [23,61—67]. Sufficient information on the underlying algorithmic concepts is mostly missing. In a positive sense, however, the multitude of application examples published so far demonstrate impressive improvements with respect to noise reduction and image quality in general. An example of a body dataset acquired with a modern clinical CT and reconstructed with both FBP and the dedicated iterative reconstruction product of the manufacturer is shown in Fig. 3. Studies comparing IR products and their state-of-the-art FBP counterparts revealed a range of dose reduction values from -7% [63], -27% [62], -35% [65], -43% [63] to -50% [23]. Other publications offer results regarding the noise reduction potentials which amounted to -13% to -21.6% [64], 40% [67] and -31.5% to -51.7% [66]. The studies investigated the IR image quality performance with whole

Figure 3 Example of body dataset of a modern clinical CT reconstructed with both FBP (a, c) and the dedicated IR product of the manufacturer (b, d) (Courtesy of Dr. M. Lell, University Erlangen-Nuremberg).

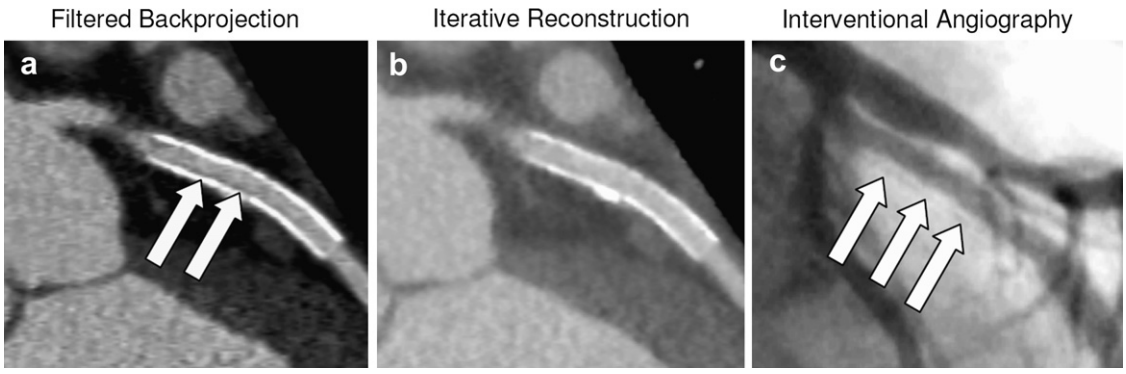

Figure 4 Can differences in image content be excluded between standard and iterative reconstruction? In the case of a coronary artery CT angiography, the standard FBP reconstruction revealed a hypodense seam along the stent indicating proliferation of the vessel intima which may ultimately lead to stent stenosis (a), This seam is not visible in IR (b), but was confirmed by interventional angiography (c). (Courtesy of Dr. S. Achenbach, University of Giessen).

body, cardiac or neurological CT scans, but the given potentials are not directly compared. It is known that noise is related inversely proportional to the square root of dose and, correspondingly, dose reduction values are higher than values for noise reduction [5]. E.g., a noise reduction by 30.8% as determined by Winklehner et al. for CT angiography [23] corresponds to a dose reduction of above 50% since, trivially, the square root of 0.308 is equal to 0.555. There is general agreement that a potential for dose reduction in the range 30–60% appears realistic and confirms earlier estimates of about 40% [5].

However, this does not necessarily mean that IR methods which reduce the image noise by a factor x can provide FBP equivalent images with identical quality and spatial resolution with dose being reduced by $1/x^2$. There are some concerns with respect to statistical modeling which is not deterministic by definition that it may cause a reduction of spatial resolution and possibly obscure details of interest. A respective example is shown in Fig. 4 where some subtle, but diagnostically important details are obscured. Note that this was only a problem of a specific IR implementation and the used set of parameters, but not a general problem of all IR methods.

The image quality performance of different IR products is hard to compare in general since they are scanner-specific and many other system parameters can also have a noteworthy

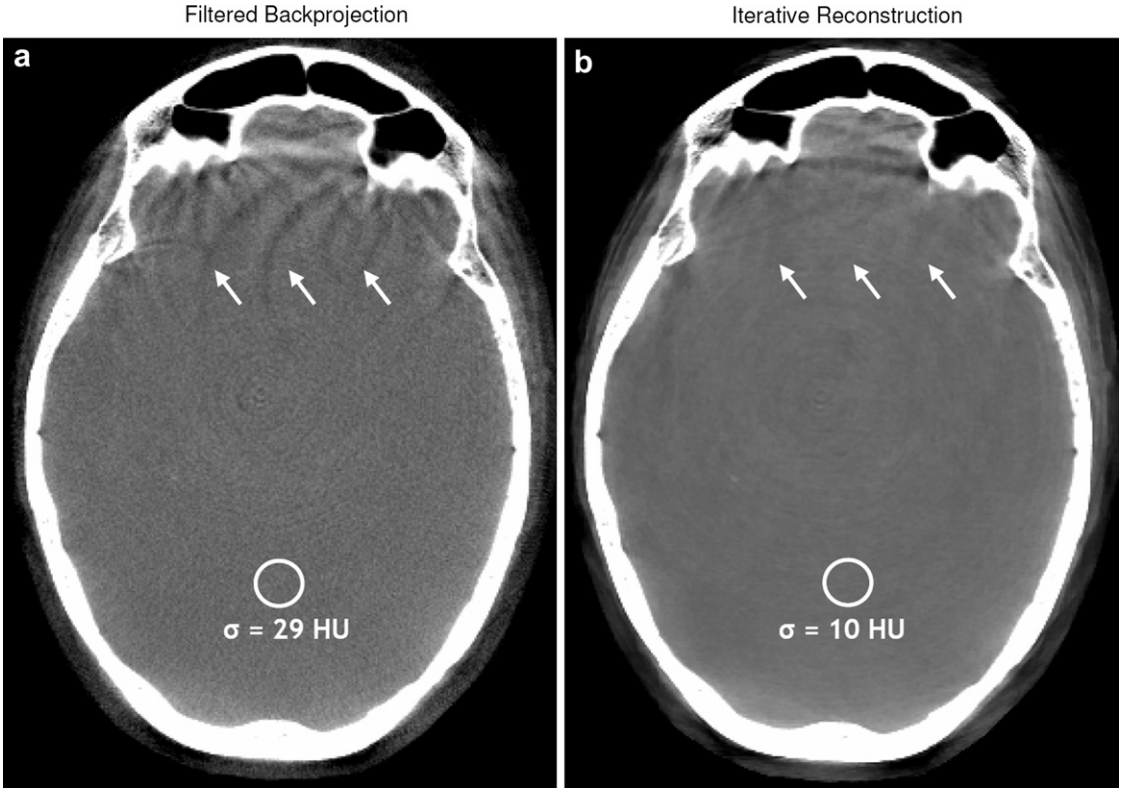

Figure 5 Comparison between FBP and MBIR reconstructions of a head scan acquired with a robotic C-arm device (C 0, W 1000). The noise in the IR image (b) is reduced by about 60% compared to the FBP results (a) without compromising spatial resolution.

influence on the reconstruction performance. At best a comparison of complete systems may be possible. There appears to be consensus, however, that MBIR approaches including geometric modeling reliably reduce noise and improve image sharpness at the same time, e.g [23,68].

Dependable information regarding the computation times are also not generally available; vendor statements vary between 1 min and 1 h depending on the scan range and on the models implemented. It can be safely assumed, however, that computation times will be reduced further in the future due to improvements of technology and implementations.

CT in general

IR approaches can be universally applied to CT scanner concepts and applications of any type. We here illustrate this fact using examples for C-arm-based flat-detector CT (FDCT), for dedicated CT of the breast, and for micro-CT applied in pre-clinical studies of mice in-vivo. All three examples were generated using the MBIR implementation described in Section: "Implementation of a model-based iterative reconstruction".

C-arm systems are often used during interventional examinations and surgeries and multiple acquisitions of the patient are done in order to evaluate the progress or success through volumetric images. This can lead to high accumulated dose levels; dose-efficient IR methods have the potential to notably reduce these levels. In comparison to clinical CT, C-arm devices are mostly restricted in terms of possible angular scan range due to the missing slip ring technology. This may lead to or can even be used for partial or short scans with data insufficient for a complete reconstruction. Due to the limited readout speed of most flat-

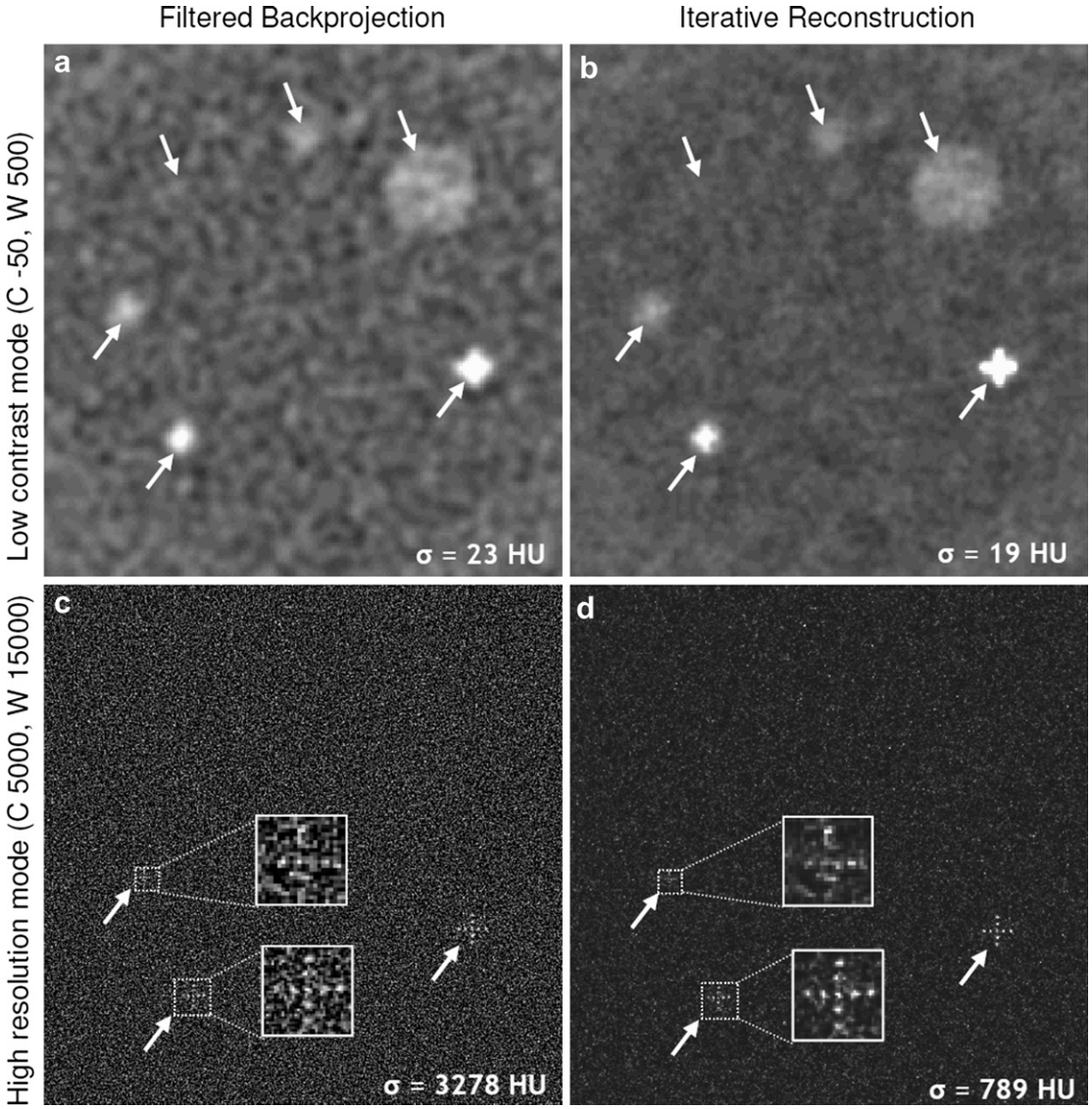

Figure 6 Comparison of breast CT simulations at 3 mGy AGD with FBP reconstruction (a, c) and MBIR (b, d). Three dimensional gauss filtration with different strength was performed on the low-contrast images (a, b) as a post-processing step to achieve similar dose levels. The IR low-contrast mode display (b) offers better resolution and the noise level is still reduced by about 20% (a). In the high-resolution mode, IR allows a noise reduction of about 75% and improvements in resolution for both 100 and 150 μm microcalcifications (d) as compared to (c).

detectors, the number of projections per scan is also limited. Iterative reconstruction methods can deal much better with incomplete or sparse data compared to FBP-based methods and easily allow incorporating prior information. In such cases improvements in image quality can be expected. Figure 5 shows an example of an FDCT brain scan acquired with a robotic C-arm device and reconstructed with both FBP and MBIR. The usage of IR reduced the noise by about 60% without compromising spatial resolution.

Dedicated CT of the breast is currently under development; details of the general concept and the expected performance were published recently [68]. The MBIR implementation presented in Section: "Implementation of a model-based iterative reconstruction" was essential in achieving the defined goal of high spatial resolution at an average glandular dose comparable to screening mammography. This was demonstrated using simulated data of breast phantoms including clusters of microcalcifications of different sizes and soft-tissue lesions in different sizes and structures of glandular tissue (Fig. 6). Three dimensional gauss filtration with different strength was performed on the low-contrast images as a post-processing step to achieve similar dose levels. MBIR allowed a reduction of noise levels in both low-contrast (60—72% without and 20% with post-processing) and high-resolution reconstruction modes (81—84%). Detectability of soft-tissue lesions was clearly improved just the same.

The MBIR algorithm was also applied to in-vivo micro-CT data sets. The example (see Fig. 7) shows a dynamic scan taken to assess and visualize the contrast enhancement within implanted mammary tumors after intravenous injection of a contrast medium bolus. The noise in the IR images was reduced by 40—50% compared to the FBP results without compromising spatial resolution.

Discussion

Iterative reconstruction algorithms have several advantages compared to analytical FBP-based methods: They allow integrating various physical models, which can reduce image noise and various artifacts depending on the degree of modeling. By modeling the causes of artifacts during the reconstruction instead of developing workarounds for their removal, iterative methods also represent the more intuitive and natural way of image reconstruction. They avoid

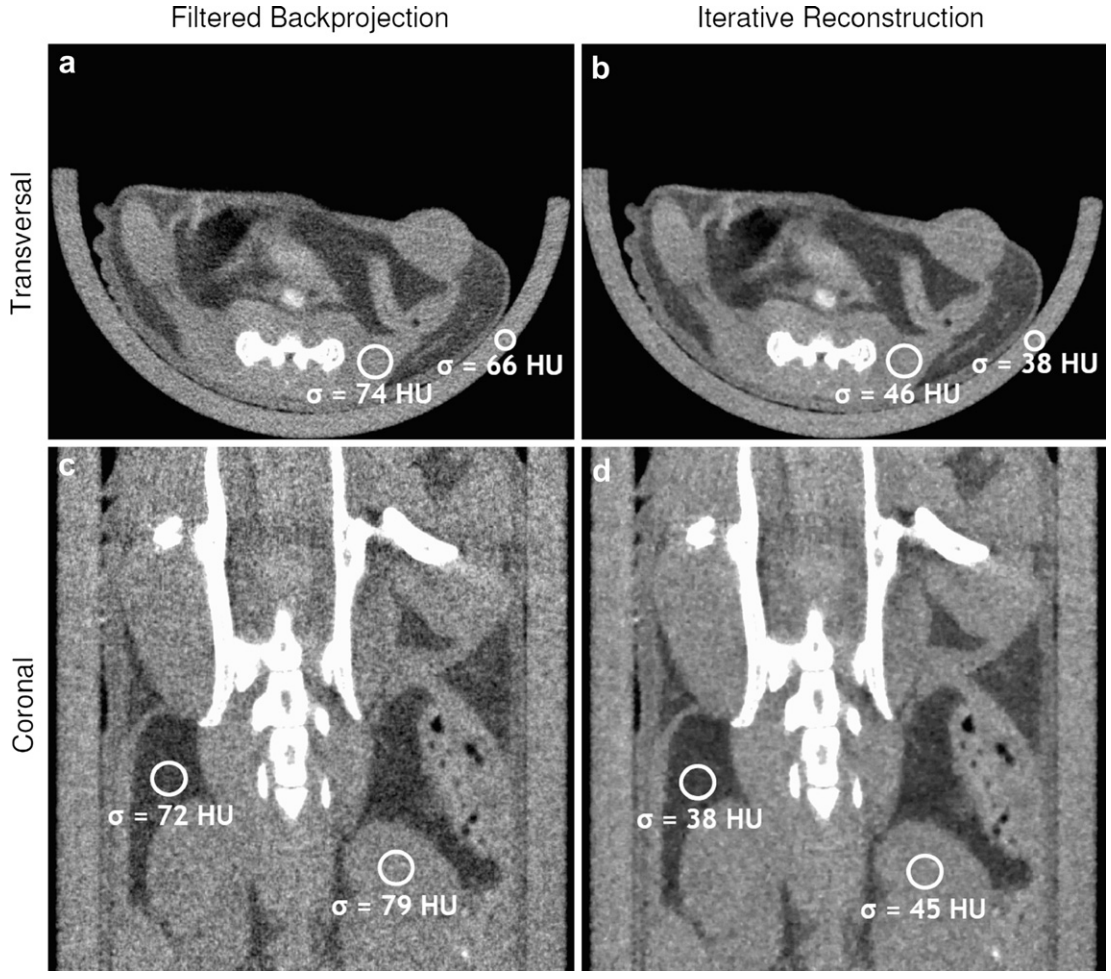

Figure 7 Comparison of FBP and MBIR results for a dynamic micro-CT scan with 65 kV tube voltage, 0.3 mA tube current and 375 projections acquired in 15 s (C 0, W 1000). The noise in the IR images (b, d) is reduced by 40—50% compared to the FBP results (a, c) without compromising spatial resolution.

introducing new artifacts due to approximations which are often used in analytical reconstruction methods and they are more suited for dealing with missing data or irregular sampling. Especially the use of prior information, such as an initial volume, can improve the image quality significantly in combination with sparse and incomplete data. In addition, iterative methods allow much higher flexibility in the scan geometry since no explicit expression of an inverse transform is necessary and therefore many different trajectories are possible, although restrictions described by the Tuy sampling criteria [69], still apply, of course.

The potential for patient dose reduction is generally considered the biggest advantage of IR methods, and applications such as pediatric CT imaging, where dose figures are of great concern, are a prime target. The literature at present abounds with studies indicating considerable dose reduction possibilities. However, there are only few official statements. So far, only two IR software products have received clearance released by the Food and Drug Administration of the USA: VEO and SAFIRE (Table 2). A claim of dose reduction was only granted for SAFIRE and amounts to 54–60% at highest noise reduction strength.

The main disadvantage of all iterative reconstruction methods lies in the increased computational effort that becomes necessary due to multiple iterations instead of a single iteration for analytical methods. In addition, a forward projection for each raw data projection becomes necessary in all iterations. Even with fast workstations and GPUs and the help of Moore's law, computing power may still be insufficient for more complex modeling of, e.g. dual energy CT, scattering, motion compensation and dynamic measurements. Iterative methods do have further downsides. For example, the reconstruction of the complete field of measurement is mandatory [70] and the evaluation of image quality parameters such as spatial resolution and noise is more complicated because they cannot be analyzed separately [71]. Also the resulting volumetric image depends on the prior information used for the parameterization of the acquisition model, and the necessary number of iterations might vary strongly depending on the measured object [50,72,73]. This makes the dose reduction potential and quantification very challenging. Also, the speed is hard to measure and to compare due to a large number of variables that influence the duration of the reconstruction process. In addition the non-linear processing during model-based IR algorithms is difficult to parameterize and may cause undesired effects as shown in Fig. 4.

Open questions refer to, for example, the statistical modeling for very low dose CT in which detector electronic effects become more dominant or the physical modeling of polychromatic interactions including scatter and beam hardening. The acceptance of iterative reconstruction methods has also been a psychological-related topic for the past years, since the reconstructed volumetric images show different noise patterns and some artifacts manifest themselves in a way different from analytical reconstruction methods. Some radiologists miss the impression they are used to, therefore some manufacturers of IR products choose to reduce the impact of this problem by blending IR results with FBP results with a user-selectable weighting factor. Moreover, noise patterns and artifacts differ from implementation to implementation. It took many years of training for radiologists to become experts in interpreting and diagnosing images from CT modalities. Switching to images of a new reconstruction method requires the radiologist to adapt. A movement away from analytical methods in favor of iterative methods can nevertheless be anticipated for CT in general within the next few years.

Conflict of interest statement

None.

Acknowledgements

The authors are grateful for the financial support of this work by the Bundesministerium für Bildung und Forschung (BMBF, Az. 01EX1002). Special thanks go to Dr. Stephan Achenbach and Dr. Michael Lell for providing the images in Section: "Clinical CT".

References

[1] Brooks RA, Chiro GD. Principles of computer assisted tomography (CAT) in radiographic and radioisotopic imaging. Phys Med Biol 1976;21:689–732.
[2] Hounsfield GN. Computerized transverse axial scanning (tomography). part I. description of system. Br J Radiol 1973; 46:1016–22.
[3] Wang G, Frei T, Vannier MW. Fast iterative algorithm for metal artifact reduction in X-ray CT. Acad Radiol 2000;7:607–14.
[4] Brenner DJ, Hall EJ. Computed tomography - an increasing source of radiation exposure. N Engl J Med 2007;357:2277–84.
[5] Kalender WA. Computed tomography: fundamentals, system technology, image quality, applications. 3rd edn. Erlangen: Publicis Publishing; 2011.
[6] Gordon R, Bender R, Herman GT. Algebraic reconstruction techniques (ART) for three-dimensional electron microscopy and x-ray photography. J Theor Biol 1970;29:471–82.
[7] Kaczmarz S. Angenäherte Auflösung von Systemen Linearer Gleichungen. Bull Internat Acad PolonSci Lettres A; 1937: 335–57.
[8] Andersen AH, Kak AC. Simultaneous algebraic reconstruction technique (SART): a superior implementation of the ART algorithm. Ultrason Imaging 1984;6:81–94.
[9] Lange K, Carson R. EM reconstruction algorithms for emission and transmission tomography. J Comput Assist Tomogr 1984;8: 306–16.
[10] Hudson HM, Larkin RS. Accelerated image reconstruction using ordered subsets of projection data. IEEE Trans Med Imaging 1994;13:601–9.
[11] Manglos SH, Gagne GM, Krol A, Thomas FD, Narayanaswamy R. Transmission maximum-likelihood reconstruction with ordered subsets for cone beam CT. Phys Med Biol 1995;40: 1225–41.
[12] Gilbert P. Iterative methods for the three-dimensional reconstruction of an object from projections. Jl Theor Biol 1972;36:105–17.
[13] Xu F, Xu W, Jones M, Keszthelyi B, Sedat J, Agard D, et al. On the efficiency of iterative ordered subset reconstruction algorithms for acceleration on GPUs. Comput Methods Programs Biomed 2010;98:261–70.
[14] Lent A, Censor Y. The primal-dual algorithm as a constraint-set-manipulation device. Math Programming 1991;50:343–57.

[15] Badea C, Gordon R. Experiments with the nonlinear and chaotic behaviour of the multiplicative algebraic reconstruction technique (MART) algorithm for computed tomography. Phys Med Biol 2004;49:1455—74.
[16] Xu J, Tsui BMW. Electronic noise modeling in statistical iterative reconstruction. IEEE Trans Image Process 2009;18:1228—38.
[17] Hsieh J. Adaptive streak artifact reduction in computed tomography resulting from excessive x-ray photon noise. Med Phys 1998;25:2139—47.
[18] Rivière PJL, Pan X. Nonparametric regression sinogram smoothing using a roughness-penalized poisson likelihood objective function. IEEE Trans Med Imaging 2000;19:773—86.
[19] Kachelriess M, Watzke O, Kalender WA. Generalized multi-dimensional adaptive filtering for conventional and spiral single-slice, multi-slice, and cone-beam CT. Med Phys 2001; 28:475—90.
[20] Rivière PJL. Penalized-likelihood sinogram smoothing for low-dose CT. Med Phys 2005;32:1676—83.
[21] Forthmann P, Köhler T, Begemann PGC, Defrise M. Penalized maximum-likelihood sinogram restoration for dual focal spot computed tomography. Phys Med Biol 2007;52:4513—23.
[22] Moscariello A, Takx RAP, Schoepf UJ, Renker M, Zwerner PL, O'Brien TX, et al. Coronary CT angiography: image quality, diagnostic accuracy, and potential for radiation dose reduction using a novel iterative image reconstruction technique-comparison with traditional filtered back projection. Eur Radiol 2011;21:2130—8.
[23] Winklehner A, Karlo C, Puippe G, Schmidt B, Flohr T, Goetti R, et al. Raw data-based iterative reconstruction in body CTA: evaluation of radiation dose saving potential. Eur Radiol 2011; 21:2521—6.
[24] Shepp LA, Vardi Y. Maximum likelihood reconstruction for emission tomography. IEEE Trans Med Imaging 1982;1:113—22.
[25] Lange K. Convergence of EM image reconstruction algorithms with Gibbs smoothing. IEEE Trans Med Imaging 1990;9:439—46.
[26] Lange K, Fessler JA. Globally convergent algorithms for maximum a posteriori transmission tomography. IEEE Trans Image Process 1995;4:1430—8.
[27] Kamphuis C, Beekman FJ. Accelerated iterative transmission CT reconstruction using an ordered subsets convex algorithm. IEEE Trans Med Imaging 1998;17:1101—5.
[28] Erdogan H, Fessler JA. Ordered subsets algorithms for transmission tomography. Phys Med Biol 1999;44:2835—51.
[29] Beekman FJ, Kamphuis C. Ordered subset reconstruction for x-ray CT. Phys Med Biol 2001;46:1835—44.
[30] Sauer K, Bouman C. A local update strategy for iterative reconstruction from projections. IEEE Trans Sig Proc 1993; 41(2):534—48.
[31] Bouman C, Sauer K. A unified approach to statistical tomography using coordinate descent optimization. IEEE Trans Image Process 1996;5:480—92.
[32] Thibault J-B, Sauer KD, Bouman CA, Hsieh JA. Three-dimensional statistical approach to improved image quality for multislice helical CT. Med Phys 2007;34:4526—44.
[33] Benson TM, De Man B, Fu L, Thibault J-B. Block-based iterative coordinate descent. In Proc IEEE Nuc Sci Symp Med Im Conf; 2010.
[34] Lee S-J. Accelerated coordinate descent methods for Bayesian reconstruction using ordered subsets of projection data. Proc SPIE Conf Math Model; 2000. 4121, pp. 170—181.
[35] Zhu H, Shu H, Zhou J, Luo L. A weighted least squares PET image reconstruction method using iterative coordinate descent algorithms. Proc. IEEE Nuclear Science Symp Conf Record; 2004. 6, pp. 3380—3384.
[36] Yu Z, Thibault J-B, Bouman CA, Sauer KD, Hsieh J. Fast model-based X-ray CT reconstruction using spatially nonhomogeneous ICD optimization. IEEE Trans Image Process 2011;20: 161—75.
[37] De Man B, Basu S. Distance-driven projection and back-projection in three dimensions. Phys Med Biol 2004;49:2463—75.
[38] Ziegler A, Köhler T, Nielsen T, Proksa R. Efficient projection and backprojection scheme for spherically symmetric basis functions in divergent beam geometry. Med Phys 2006;33: 4653—63.
[39] Long Y, Fessler JA, Balter JM. 3D forward and back-projection for X-ray CT using separable footprints. IEEE Trans Med Imaging 2010;29:1839—50.
[40] Peters TM. Algorithms for fast back- and re-projection in computed tomography. IEEE Trans Nucl Sci 1981;28:3641—7.
[41] Joseph PM. An improved algorithm for reprojecting rays through pixel images. IEEE Trans Med Imaging 1982;1:192—6.
[42] Siddon RL. Fast calculation of the exact radiological path for a three-dimensional CT array. Med Phys 1985;12:252—5.
[43] Chou C-Y, Chuo Y-Y, Hung Y, Wang W. A fast forward projection using multithreads for multirays on GPUs in medical image reconstruction. Med Phys 2011;38:4052—65.
[44] Sohlberg A, Watabe H, Zeniya T, Iida H. Comparison of multi-ray and point-spread function based resolution recovery methods in pinhole SPECT reconstruction. Nucl Med Commun 2006;27:823—7.
[45] Moehrs S, Defrise M, Belcari N, Del Guerra A, Bartoli A, Fabbri S, et al. Multi-ray-based system matrix generation for 3D PET reconstruction. Phys Med Biol 2008;53:6925—45.
[46] Tucker DM, Barnes GT, Chakraborty DP. Semiempirical model for generating tungsten target x-ray spectra. Med Phys 1991; 18:211—8.
[47] De Man B, Nuyts J, Dupont P, Marchal G, Suetens P. An iterative maximum-likelihood polychromatic algorithm for CT. IEEE Trans Med Imaging 2001;20:999—1008.
[48] Elbakri IA, Fessler JA. Statistical image reconstruction for polyenergetic X-ray computed tomography. IEEE Trans Med Imaging 2002;21:89—99.
[49] Elbakri IA, Fessler JA. Segmentation-free statistical image reconstruction for polyenergetic x-ray computed tomography with experimental validation. Phys Med Biol 2003;48:2453—77.
[50] Xu W, Mueller K. A performance-driven study of regularization methods for GPU-accelerated iterative CT. Proc 2nd High Performance Image Reconstruction Workshop; 2009.
[51] Xu W, Mueller K. Evaluating popular non-linear image processing filters for their use in regularized iterative CT. IEEE Trans Med Imaging; 2010:2864—5.
[52] Rudin LI, Osher S, Fatemi E. Nonlinear total variation based noise removal algorithms. Physica D: Nonlinear Phenomena 1992;60:259—68.
[53] Zhu M, Wright S, Chan T. Duality-based algorithms for total-variation-regularized image restoration. Compu Optim Appl 2010;47:377—400.
[54] Tian Z, Jia X, Yuan K, Pan T, Jiang SB. Low-dose CT reconstruction via edge-preserving total variation regularization. Phys Med Biol 2011;56:5949—67.
[55] Bouman C, Sauer K. A generalized Gaussian image model for edge-preserving MAP estimation. IEEE Trans Image Process 1993;2:296—310.
[56] Ziegler A, Köhler T, Proksa R. Noise and resolution in images reconstructed with FBP and OSC algorithms for CT. Med Phys 2007;34:585—98.
[57] Kole JS, Beekman FJ. Evaluation of the ordered subset convex algorithm for cone-beam CT. Phys Med Biol 2005;50:613—23.
[58] Pock T, Unger M, Cremers D, Bischof H. Fast and exact solution of total variation models on the GPU. Comp. Vis. Patt. Reco; 2008. pp. 1—8.
[59] Chan TF, Golub GH, Mulet P. A nonlinear primal-dual method for total variation-based image restoration. SIAM J Appl Math 1999;20:1964—77.
[60] Chambolle A. An algorithm for total variation minimization and applications. J Math Imaging Vis 2004;20:89—97.

[61] Singh S, Kalra MK, Hsieh J, Licato PE, Do S, Pien HH, et al. Abdominal CT: comparison of adaptive statistical iterative and filtered back projection reconstruction techniques. Radiology 2010;257:373—83.
[62] Leipsic J, Labounty TM, Heilbron B, Min JK, Mancini GBJ, Lin FY, et al. Estimated radiation dose reduction using adaptive statistical iterative reconstruction in coronary CT angiography: the ERASIR study. AJR Am J Roentgenol 2010;195:655—60.
[63] Leipsic J, Labounty TM, Heilbron B, Min JK, Mancini GBJ, Lin FY, et al. Adaptive statistical iterative reconstruction: assessment of image noise and image quality in coronary CT angiography. AJR Am J Roentgenol 2010;195:649—54.
[64] Bittencourt MS, Schmidt B, Seltmann M, Muschiol G, Ropers D, Daniel WG, et al. Iterative reconstruction in image space (IRIS) in cardiac computed tomography: initial experience. Int J Cardiovasc Imaging 2010;27:1081—7.
[65] Pontana F, Pagniez J, Flohr T, Faivre J-B, Duhamel A, Remy J, et al. Chest computed tomography using iterative reconstruction vs filtered back projection (part 1): evaluation of image noise reduction in 32 patients. Eur Radiol 2011;21: 627—35.
[66] Pontana F, Duhamel A, Pagniez J, Flohr T, Faivre J-B, Hachulla A-L, et al. Chest computed tomography using iterative reconstruction vs filtered back projection (part 2): image quality of low-dose CT examinations in 80 patients. Eur Radiol 2011;21:636—43.
[67] Gervaise A, Osemont B, Lecocq S, Noel A, Micard E, Felblinger J, et al. CT image quality improvement using adaptive iterative dose reduction with wide-volume acquisition on 320-detector CT. Eur Radiol; 2011. published online.
[68] Kalender WA, Beister M, Boone JM, Kolditz D, Vollmar SV, Weigel MCC. High-resolution spiral CT of the breast at very low dose: concept and feasibility considerations. Eur Radiol 2012; 22:1—8.
[69] Tuy HK. An inversion formula for cone-beam reconstruction. SIAM J Appl Math 1983;43:546—52.
[70] Ziegler A, Nielsen T, Grass M. Iterative reconstruction of a region of interest for transmission tomography. Med Phys 2008;35:1317—27.
[71] Liow JS, Strother SC. The convergence of object dependent resolution in maximum likelihood based tomographic image reconstruction. Phys Med Biol 1993;38:55—70.
[72] Zbijewski W, Beekman FJ. Suppression of intensity transition artifacts in statistical x-ray computer tomography reconstruction through radon inversion initialization. Med Phys 2004;31:62—9.
[73] Xu J, Mahesh M, Tsui BMW. Is iterative reconstruction ready for MDCT? J Am Coll Radiol 2009;6:274—6.